



CrossMark  
click for updates

Cite this: *RSC Adv.*, 2016, 6, 13478

# Synthesis and characterization of highly fluorinated sulfonated polytriazoles for proton exchange membrane application

Asheesh Singh,<sup>a</sup> Susanta Banerjee,<sup>\*a</sup> Hartmut Komber<sup>b</sup> and Brigitte Voit<sup>b</sup>

A series of polytriazole copolymers (PTFQSH-XX) were synthesized by the click polymerization of 1,1,1,3,3,3-hexafluoro-2,2-bis(4-(prop-2-ynoxy)phenyl)propane (TF) with a mixture of two diazide monomers: 4,4-bis[3-trifluoromethyl-4(4-azidophenoxy)phenyl]biphenyl (QAZ) and 4,4'-diazido-2,2'-stilbene disulfonic acid disodium salt ("S"). The degree of sulfonation (DS) of the copolymers was controlled by adjusting the mole ratio of "S" to the non-sulfonated diazide (QAZ). The polytriazole copolymers were characterized by FTIR and NMR (<sup>1</sup>H, <sup>13</sup>C and <sup>19</sup>F) spectroscopy. The PTFQS-XX membranes were prepared by dissolving the salt form of the copolymers in dimethyl formamide. The physical properties and proton conductivity of the membranes were investigated. The presence of hexafluoroisopropylidene groups in the copolymers contributed to high thermal and oxidative stability and low swelling of the membranes. TEM micrographs of the polytriazole membranes showed a good phase separated morphology with ionic clusters in the range of 3–75 nm. The proton conductivities of the fluorinated membranes were found in the range of 27–136 mS cm<sup>-1</sup> at 80 °C in water.

Received 15th December 2015  
Accepted 21st January 2016

DOI: 10.1039/c5ra26821d

www.rsc.org/advances

## 1. Introduction

Proton exchange membrane fuel cells (PEMFCs) have received increasing attention in the past decades as both automotive and portable electronic applications due to their high energy efficiency, low emission pollutants, and simple operation.<sup>1</sup> Proton exchange membranes in PEMFCs play an important role as an electrolyte, which conducts the proton, and acts as a barrier between the fuel and oxygen. At present, perfluoro sulfonic acid (PFSA) ionomers, such as Nafion®, are commonly used as proton exchange membranes in PEMFCs because of their high proton conductivity in combination with outstanding chemical and physical properties. However, the cost, high methanol permeability, and loss of proton conductivity at high temperature hinder the widespread applications of Nafion®117.<sup>2</sup> To overcome all these problems, a large number of sulfonated aromatic polymers were synthesized as important PEM materials such as sulfonated poly(arylene ether sulfone)s,<sup>3–6</sup> sulfonated poly(ether ether ketone)s,<sup>7–10</sup> sulfonated polyimides,<sup>11–14</sup> sulfonated poly(benzimidazole)s,<sup>15–17</sup> and sulfonated polytriazoles.<sup>18–21</sup>

In recent years, the copper-catalyzed azide-alkyne click chemistry (CuAAC) reactions have been widely used in the preparation of polymers, due to their remarkable features such as near perfect

reliability, high yield, mild reaction conditions, tolerance towards a wide range of functional groups and simple product isolation.<sup>22–24</sup> This technique has been widely utilized in the synthesis of linear polymers, block copolymers, graft copolymers, hyperbranched polymers and crosslinked polymers, but so far it has not been much used for the synthesis of sulfonated polymers.<sup>25–29</sup> A better oxidative and hydrolytic stability of polytriazoles is expected in comparison to the hetero-chain polymers, due to the presence of a stable aromatic triazole ring.<sup>18</sup> In general, the proton conductivity of polymers can be improved by increasing the concentration of the sulfonic acid groups. However, this approach results in excessive water swelling and consequently strongly reduced mechanical properties, and hence the membranes are not suitable for proton exchange membrane applications. Incorporation of fluorine in the polymers is an effective approach to improve the mechanical, thermal and chemical stabilities. Also, the presence of fluorine helps in getting phase segregated morphology, which finally improves the proton conduction<sup>30,31</sup> compared to that of non-fluorinated analogue. By taking these indications into account, our group prepared and characterized a series of sulfonated fluorinated polytriazole copolymers (PTAQSH-XX) with varying degree of sulfonation by the click reaction of a new diazido monomer; 4,4-bis[3-trifluoromethyl-4(4-azidophenoxy)phenyl]biphenyl and 4,4'-diazido-2,2'-stilbene disulfonic acid disodium salt with 4,4'-(propane-2,2-diyl)bis((prop-2-ynoxy)benzene) (BPEBPA) in a first study.<sup>21</sup>

In continuation of this study, in this work we want to investigate the effect of increased fluorine content on the PEM properties by using highly fluorinated monomers. Accordingly,

<sup>a</sup>Materials Science Centre, Indian Institute of Technology, Kharagpur 721302, India. E-mail: susanta@matssc.iitkgp.ernet.in; Fax: +91-3222-255303; Tel: +91-3222-283972

<sup>b</sup>Leibniz-Institut für Polymerforschung Dresden e.V., Hohe Strasse. 6, 01067 Dresden, Germany

we have synthesized a fluorinated di-alkyne monomer containing hexafluoroisopropylidene  $\text{>C}(\text{CF}_3)_2$  moiety. Using this monomer, a series of highly sulfonated polytriazole copolymers (PTFQSH-XX) with varying degree of sulfonation was prepared by click polymerization of 4,4-bis[3-trifluoromethyl-4(4-azidophenoxy)phenyl] biphenyl (QAZ), 4,4'-diazido-2,2'-stilbene disulfonic acid disodium salt ("S") and 1,1,1,3,3,3-hexafluoro-2,2-bis(4-(prop-2-ynoxy)phenyl)propane (TF). PTFQSH-XX copolymers are expected to show better phase separation, low water uptake, low swelling, relatively high oxidative stability and high proton conductivity, in comparison to the PTAQSH-XX series, due to the presence of both, hydrophobic trifluoromethyl ( $-\text{CF}_3$ ) and  $\text{>C}(\text{CF}_3)_2$  groups.<sup>7,11,31,32</sup> The structures of the PTFQSH-XX copolymers were characterized by NMR and FTIR spectroscopy. The PEM properties of the prepared sulfonated polytriazoles were studied, such as proton conductivity, mechanical properties, thermal stability, water uptake and swelling ratio.

## 2. Experimental

### 2.1. Materials

4,4'-(Hexafluoroisopropylidene)-diphenol (BPF) (95% purity) was purchased from Fluorochem, UK, *tert*-butylnitrite (*t*-BuONO), azidotrimethylsilane ( $\text{TMSN}_3$ ), propargyl bromide and 4,4'-diazido-2,2'-stilbene disulfonic acid disodium salt hydrate ("S") were purchased from Aldrich, USA, and were used as received. Copper(I)

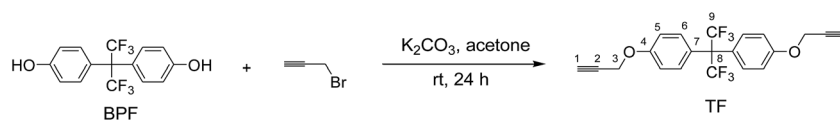
iodide, potassium carbonate and *N,N*-dimethylformamide (DMF) were purchased from Spectrochem, India, and were used as received. Concentrated sulfuric acid (95%), acetonitrile ( $\text{CH}_3\text{CN}$ ), and ammonia solution (25%) were purchased from E. Merck, India. 4,4-Bis[3-trifluoromethyl-4(4-aminophenoxy)phenyl]biphenyl (QAZ) was prepared according to our previous article.<sup>21</sup>

### 2.2. Synthesis of TF monomer

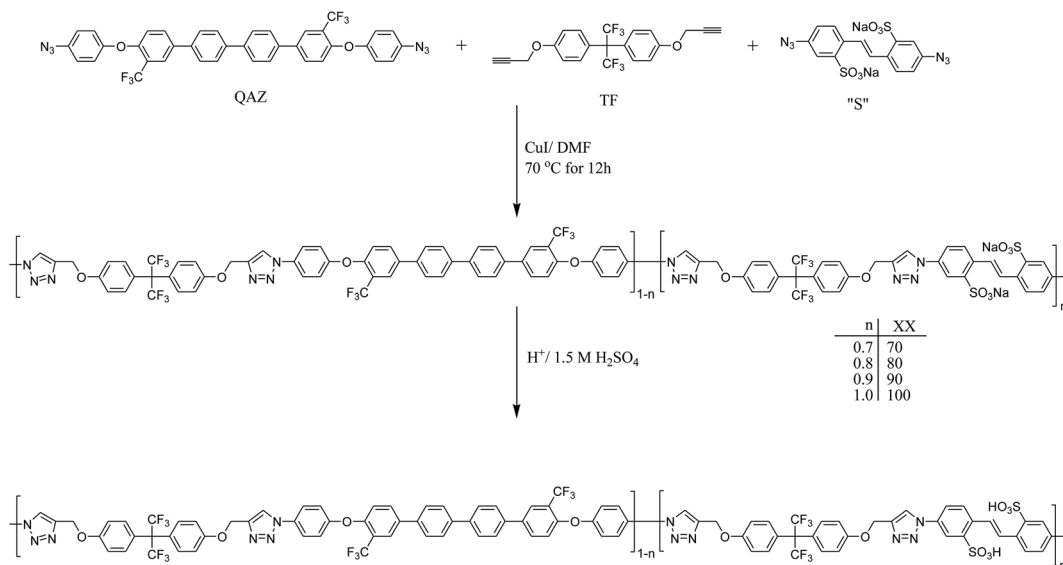
The fluorinated dialkyne was synthesized using a modified method from corresponding diphenol according to the Scheme 1.

A 250 mL three-necked round bottom flask equipped with a nitrogen inlet, refluxing condenser and a magnetic stirrer was charged with 4,4'-(hexafluoroisopropylidene)-diphenol (9.30 g, 27.65 mmol), anhydrous potassium carbonate (15.29 g, 110.59 mmol), 80 mL dry acetone and the reaction mixture was stirred at room temperature for 30 minutes. To this reaction mixture, propargyl bromide (8.23 g, 69.12 mmol) was added dropwise over 1 h and the reaction mixture was stirred at room temperature for another 24 h. The reaction mixture was washed several times with deionized water to remove excess potassium carbonate and the salt formed (KBr) in the reaction. The product was extracted with ethyl acetate and dried in vacuum at 70 °C for 12 h. Finally, a pale yellow viscous liquid was obtained as a product.<sup>33</sup> Yield: 9.7 g (~85%).

<sup>1</sup>H NMR (DMSO- $d_6$ ): 7.27 (6), 7.09 (5), 4.85 (3), 3.60 ppm (1).  
<sup>13</sup>C NMR (DMSO- $d_6$ ): 157.7 (4), 130.9 (6), 124.9 (7), 123.2 (q, <sup>1</sup>J<sub>CF</sub>



Scheme 1 Synthesis of the dialkyne monomer TF.



Scheme 2 Synthesis of PTFQSH-XX copolymers.

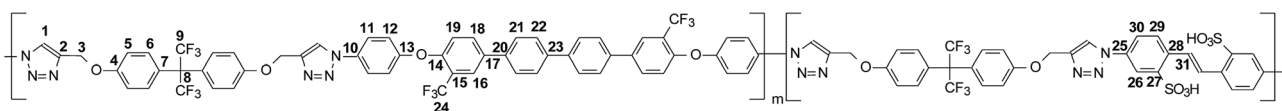
= 287 Hz; 9), 114.8 (5), 78.8 (2), 78.5 (1), 63.1 (sept,  $^2J_{CF} = 25$  Hz; 8), 55.6 ppm (3).  $^{19}\text{F}$  NMR (DMSO- $d_6$ ): -64.2 ppm.

### 2.3. Synthesis of sulfonated polytriazoles

**2.3.1. Preparation of homopolymers (PTFQ and PTFSH-100) and copolymers (PTFQSH-XX).** The polytriazoles PTFQSH-XX (where XX is the mole percentage of the sulfonated comonomer "S" in the diazide mixture) were prepared by click polymerization as shown in Scheme 2.

The salt form and the acid form are denoted as PTFQS-XX and PTFQSH-XX, respectively. A typical procedure, for the preparation of the PTFQS-70 copolymer is described below. QAZ (0.2234 g, 0.31 mmol), TF (0.4334 g, 1.05 mmol), "S" (0.3961 g, 0.73 mmol), CuI (0.1 g, 0.052 mmol) and DMF (12 mL) were placed in a 50 mL completely dried three-necked round bottom flask equipped with a magnetic stirrer, reflux condenser, and nitrogen inlet. The reaction mixture was heated to 70 °C under stirring and  $\text{N}_2$  flow condition for 12 h. The polymer solution was cooled to room temperature and was precipitated with isopropanol. The yellow fibrous polymer was obtained by vacuum filtration, thoroughly washed with 20% ammonia solution followed by deionized water, and dried under vacuum at 100 °C for 12 h. The yield was 99%.

#### PTFQSH-XX.

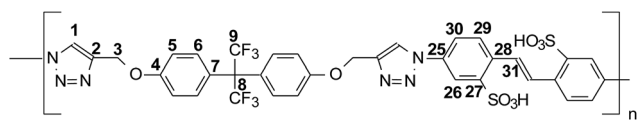


$^1\text{H}$  NMR (DMSO- $d_6$ , 90 °C): 8.85–8.75 (1), 8.36 (26), 8.34 (31), 8.08 (16), 8.03 (18), 7.95 (11), 7.9–7.8 (21, 22, 29, 30), 7.4–7.25 (6, 12, 19), 7.21 (5), 5.32 ppm (3).

$^{13}\text{C}$  NMR (DMSO- $d_6$ , 60 °C): 158.4 and 158.3 (4), 156.1 (13), 153.1 (14), 147.3 (27), 143.5 and 143.4 (2), 138.7 (23), 137.0 (20), 135.6 (17), 135.1 (28), 134.5 (25), 132.7 (10), 132.3 (18), 130.8 (6), 127.7 (31), 127.1 and 127.0 (21, 22), 126.9 (29), 124.9 (16), 124.5 (7), 123.9 (q,  $^1J_{CF} = 287$  Hz; 9), 123.1 (q,  $^1J_{CF} = 273$  Hz; 24), 122.8 and 122.6 (1), 122.3 (11), 120.7 (19), 120.6 (q,  $^2J_{CF} = 30$  Hz; 15), 120.3 (30), 119.5 (12), 118.8 (26), 114.7 (5), 61.2 (3), 63.0 ppm (sept,  $^2J_{CF} = 25$  Hz; 8).

$^{19}\text{F}$  NMR (DMSO- $d_6$ , 60 °C): -60.0 (24), -63.1 ppm (splitting due to different BPF centred triads; 9).

#### PTFQSH-100.



$^1\text{H}$  NMR (DMSO- $d_6$ , 90 °C): 8.83 (1), 8.36 (26), 8.34 (31), 7.88 (AB spin system; 29, 30), 7.34 (6), 7.22 (5), 5.32 ppm (3).

$^{13}\text{C}$  NMR (DMSO- $d_6$ , 60 °C): 158.4 (4), 147.1 (27), 143.5 (2), 135.0 (28), 134.5 (25), 130.8 (6), 127.7 (31), 126.9 (29), 124.5 (7), 124.0 (q,  $^1J_{CF} = 287$  Hz; 9), 122.6 (1), 120.4 (30), 118.8 (26), 114.7 (5), 61.2 (3), 63.1 ppm (sept,  $^2J_{CF} = 25$  Hz; 8).

$^{19}\text{F}$  NMR (DMSO- $d_6$ , 60 °C): -63.1 ppm (9).

**2.3.2. Membrane preparation and acidification.** The PTFQS-XX membranes were prepared by dissolving the salt form of the copolymers in DMF (10%, w/v). The resulting polymer solutions were filtered and transferred onto flat bottom Petri dishes and dried in an oven by sequential heating at 80 °C (24 h), 100 °C, 120 °C, 140 °C each for two hours and at 155 °C for 15 minutes. The membranes were finally vacuum-dried at 120 °C for 24 h. The membranes were removed from the Petri dishes by immersing them in water. Flexible and transparent yellow membranes were obtained. The average thickness of the membranes was found in the range of 50–75  $\mu\text{m}$ . The salt forms of the membranes were converted to the acid form by immersing the membranes in 1.5 M sulfuric acid for 24 h. The acid form membranes were washed thoroughly with deionized water to drain out excess acid, and finally dried under vacuum at 100 °C for 24 h.

### 2.4. Measurements and characterization

Elemental carbon, hydrogen and nitrogen of the compounds were analyzed by the pyrolysis method using a elemental

analyzer instrument (Euro Vector, EA, Italy).  $^1\text{H}$  (500.13 MHz),  $^{13}\text{C}$  (125.76 MHz) and  $^{19}\text{F}$  (470.59 MHz) NMR spectra of the sulfonated polymers were recorded on an Avance III 500 NMR spectrometer (Bruker, Germany) at 60 °C ( $^{13}\text{C}$ ,  $^{19}\text{F}$ ) and 90 °C ( $^1\text{H}$ ), respectively. To ensure full  $^1\text{H}$  relaxation a pulse delay of 60 s was applied in the  $^1\text{H}$  NMR measurements. The monomers were measured at 30 °C. The spectra were referenced on the solvent signal (DMSO- $d_6$ :  $\delta(^1\text{H}) = 2.50$  ppm,  $\delta(^{13}\text{C}) = 39.6$  ppm). The  $^{19}\text{F}$  NMR spectra were referenced on external  $\text{C}_6\text{F}_6$ . The signal assignments were confirmed by  $^1\text{H}$ - $^1\text{H}$  and  $^1\text{H}$ - $^{13}\text{C}$  correlated spectra. FTIR spectra of the copolymers were recorded from a NEXUS 870 FTIR (Thermo Nicolet) spectrophotometer at room temperature and humidity free atmosphere. The molecular weight of polymers was measured by size-exclusion chromatography (SEC) using DMAc with 3 g  $\text{L}^{-1}$  LiCl as eluent. Sample concentration was 1 mg  $\text{mL}^{-1}$ . The apparatus consists of a Gynkotek HPLC pump, an Agilent Autosampler 1200, linear columns [All GRAM, Polymer Standards Service (PSS)] consisting of a pre-column 10  $\mu\text{m}/8$  mm  $\times$  50 mm, a column 10  $\text{\AA}/8$  mm  $\times$  300 mm and two columns 3000  $\text{\AA}/8$  mm  $\times$  300 mm. A refractive-index (RI) detector of Knauer was used as a detector. For

calibration, linear PMMA with molecular weights between 500 and 1 000 000 Da was used. DSC measurement was carried out using TA Instruments, DSC (Q20) instrument at a heating rate of 10 K min<sup>-1</sup> under nitrogen. Glass transition temperature ( $T_g$ ) was taken as the middle point of the step transition in the second heating run. Thermogravimetric (TGA) analysis was performed under air using TA Instruments, TGA (Q50) instrument in the synthetic air (N<sub>2</sub>/O<sub>2</sub>: 80/20) at a heating rate of 10 K min<sup>-1</sup>. Wide angle X-ray diffraction study (WAXD) was conducted for dry and wet membrane by using RIGAKU, ULTEMA III X-ray diffractometer using a Cu K<sub>α</sub> (0.154 nm) source, operated at 40 kV and 40 mA within the range of 2 theta was 10–40°. Transmission electron microscopy (TEM) was undertaken for ultra-microtome membranes using a TEM instrument (FEI-TECNAI G2 20 S-TWIN) operated at an accelerating voltage of 80 kV. First, the acid form of the membranes was stained and converted into Pb<sup>2+</sup> form by immersing them in 0.5 M Pb(CH<sub>3</sub>-COO)<sub>2</sub> × 3H<sub>2</sub>O aqueous solution for overnight, washed thoroughly with deionized water and dried at room temperature for 24 h. Then, the samples were ultramicrotome under cryogenic condition with a thickness of 100 nm and were transferred onto a carbon-coated copper grids for TEM analysis. The ion exchange capacity (IEC<sub>w</sub>) was represented as the molar equivalents of ion conductor per mass of dry membrane, or milliequivalents of ion per gram (meq g<sup>-1</sup>) of polymer ( $E_w = 1000/\text{IEC}_w$ ) sample and calculated from the relationship  $\text{IEC}_w = (1000/M_w \text{ repeat unit}) \times \text{DS} \times 2$ ; where DS is the degree of sulfonation. The IEC<sub>w</sub> values of the acid form membranes were also determined by the acid–base titration method using the relationship  $\text{IEC}_w = cV(100/w)$ , where  $w$  is the weight of the dry membrane, and  $c$  and  $V$  are the concentration and volume of NaOH respectively. IEC<sub>v</sub> (dry and wet) values of the membranes were also calculated by multiplying the density of the membranes with IEC<sub>w</sub> and by considering the water uptake of the membranes respectively. The water uptake, swelling ratio and oxidative stability of the membranes were determined according to the reported protocol.<sup>21,30,34</sup> The in-plane proton conductivity (in plane) of the polymer membranes was determined by measuring the resistance ( $R$ ) value using electrochemical impedance spectroscopy (GAMRY reference 3000™) over a frequency range of 100 Hz to 1 MHz using a homemade two probe conductivity cell. The membrane between the two electrodes was allowed to equilibrate in deionized water (100% relative humidity) during experiments.

### 3. Results and discussion

#### 3.1. Synthesis of monomers

Hexafluoroisopropylidene group [ $\text{C}(\text{CF}_3)_2$ ] based bisalkyne monomer TF was prepared by the etherification reaction as shown in the Scheme 1. The fluorinated diazide monomer QAZ was prepared as described in our previous article.<sup>21</sup> The structures of the both monomers were confirmed by FTIR and <sup>1</sup>H NMR analysis. The characteristic strong absorption band around 3300 cm<sup>-1</sup> and 2123 cm<sup>-1</sup> were assigned to the stretching vibration of the  $\equiv\text{C}-\text{H}$  and  $-\text{C}\equiv\text{C}-$ , respectively, in case of TF, whereas strong absorption band around 2119 cm<sup>-1</sup> was due to the stretching vibration of azide ( $-\text{N}_3$ ) of QAZ.

#### 3.2. Synthesis of PTFQSH-XX copolymers

The salt form of the polytriazole copolymers was synthesized by the click polymerization of fluorinated dialkyne monomer TF with the stoichiometric amounts of the diazide sulfonated monomer, “S” and non-sulfonated diazide monomer, QAZ, in the presence of CuI in dry DMF as reported earlier.<sup>21</sup> The degree of sulfonation was controlled by adjusting the molar ratio of “S” to QAZ. The reaction was carried out in a nitrogen atmosphere at 70 °C for 12 h. The resultant viscous solution was diluted with DMF (~10%) and precipitate out in isopropanol. The fibrous polymers as obtained after precipitation were washed with 20% ammonia solution followed by deionized water to remove the salt impurities and dried at 100 °C under vacuum for 24 h. The membranes in the salt forms were cast from their DMF solution and converted to the acid form by sulfuric acid treatment. The copolymers (PTFQSH-XX) showed number average molecular weights ( $M_n$ ) in the range of 16 300–24 500 g mol<sup>-1</sup> with polydispersity indices ( $D$ ) in the range of 2.96–4.52. Though the  $M_n$  of the copolymers showed a decreasing trend with the increase of the DS values, the inherent viscosity values of the copolymers increased with the DS values. This is somewhat difficult to explain. Due to the electrolyte nature, the chances of interaction of the PTFQSH-XX copolymers with the column materials are very high and was evident from the broad elution peaks in the chromatograms. Thus, the SEC molecular weights of these sulfonated copolymers should be viewed with skepticism. The molar compositions of the polymers are summarized in Table 1.

#### 3.3. Characterization of PTFQSH-XX membranes

The FTIR spectra of the PTFQS-XX copolymers (salt form) are shown in Fig. 1. The disappearance of the stretching bands around 3300 cm<sup>-1</sup> and 2123 cm<sup>-1</sup> and 2119 cm<sup>-1</sup> confirmed the formation of the polytriazoles. In addition, all polymers exhibited an absorption band around at 1610 cm<sup>-1</sup> due to the aromatic C=C band and 1241–1131 cm<sup>-1</sup> due to the C-F stretching band. The characteristic aromatic sodium sulfonate (O=S=O) asymmetric stretching band around 1080 cm<sup>-1</sup> and symmetric stretching band around 1017 cm<sup>-1</sup> were also found in all sulfonated copolymers.

Despite the FTIR data confirm the general structural features of the copolymers, a more detailed and quantitative insight into the structure was possible by NMR spectroscopy. Fig. 2 depicts the <sup>1</sup>H NMR (left) and <sup>19</sup>F NMR spectra (right) of the sulfonated copolymers PTFQS-XX (XX = 70 (a)–90 (c)) and PTFSH-100 (d). The decreasing content of comonomer Q can be followed both by decreasing intensity of proton signals 11, 16 and 18, respectively, and by decreasing intensity of the CF<sub>3</sub> signal at –60.0 ppm (F<sub>24</sub>). The copolymer composition and the DS value were determined from the signal intensities of H<sub>1</sub> (TF), H<sub>26</sub> and H<sub>31</sub> (SH), and H<sub>16</sub> and H<sub>18</sub> (Q) (Table 1). The <sup>19</sup>F NMR signal integrals of F<sub>9</sub> and F<sub>24</sub> confirm the TF to Q ratio. Signals of low intensity, e.g. at 7.15 ppm in the <sup>1</sup>H NMR spectra and at –63.15 ppm in the <sup>19</sup>F NMR spectra, indicate end groups. This corresponds with the medium molecular weight determined for all samples (Table 1). The <sup>13</sup>C NMR spectrum of PTFQS-XX (not shown) resembles the spectrum of PTAQSH-XX.<sup>21</sup> The most

Table 1 Composition and properties of PTFQSH-XX copolymers

Polymer	Percentage of "S" (mmol)	$M_n^a$	$D^b$	$\eta_{inh}^c$ (dL g <sup>-1</sup> )	Elemental analysis				DS ( $\times 2$ )	
					C calcd (found)	H calcd (found)	S calcd (found)	N calcd (found)	Theo. <sup>d</sup>	NMR <sup>e</sup>
PTFQ	0	—	—	—	63.16 (63.29)	3.21 (3.23)	0	7.49 (7.52)	0	0
PTFQSH-70	70	24 500	2.96	1.52	55.01 (55.12)	3.00 (3.02)	4.87 (4.95)	9.13 (9.21)	1.40	1.40
PTFQSH-80	80	19 900	3.55	1.56	53.55 (53.61)	2.96 (2.98)	5.74 (5.82)	9.42 (9.55)	1.60	1.60
PTFQSH-90	90	19 300	4.33	1.63	51.98 (52.07)	2.92 (2.94)	6.67 (6.73)	9.73 (9.82)	1.80	1.74
PTFSH-100	100	16 300	4.52	1.72	50.32 (50.45)	2.88 (2.90)	7.67 (7.75)	10.06 (10.18)	2.00	2.00

<sup>a</sup>  $M_n$ , number average molecular weight. <sup>b</sup>  $D$ , poly dispersity index. <sup>c</sup> Inherent viscosity of PTFQSH-XX copolymers in NMP at 30 °C. <sup>d</sup> Degree of sulfonation, calculated from the monomer feed ratio. <sup>e</sup> Calculated from <sup>1</sup>H NMR signal intensities.

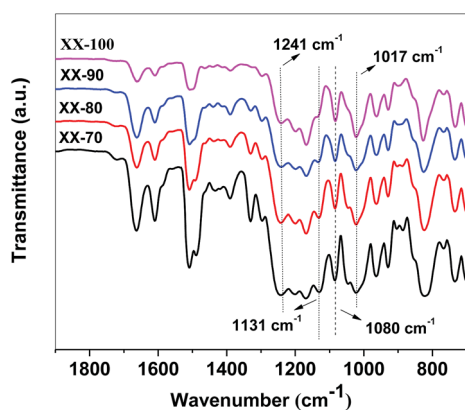


Fig. 1 FT-IR spectra of PTFQSH-XX copolymers with different degrees of sulfonation.

remarkable difference is signal splitting for C<sub>6</sub>–C<sub>9</sub> due to <sup>J</sup><sub>CF</sub> couplings. Of course, replacing –CH<sub>3</sub> by –CF<sub>3</sub> in position 9 also results in chemical shift changes for this comonomer (see Experimental). Typical for copolymers, some <sup>13</sup>C NMR signals show a splitting due to microstructure effects. Such a diad and triad splitting is also observed for the <sup>1</sup>H NMR signal 1 and the <sup>19</sup>F NMR signal 9. However, the signal separation is too small to allow a reliable quantification of microstructural units.

### 3.4. Polymer solubility

The solubility of the PTFQSH-XX copolymers was tested in several organic solvents such as NMP, DMSO, DMF, DMAc, DCM, THF and methanol. The concentration of the polymer solutions was maintained ~10% (w/v). All the PTFQSH-XX copolymers were soluble in polar aprotic organic solvents such NMP, DMF, DMAc and DMSO, and were insoluble in THF, DCM, methanol and water.

### 3.5. Thermal and mechanical properties, oxidative stability

Thermal properties of the copolymers were examined by measuring the glass transition temperature and decomposition temperatures from differential scanning calorimetry (DSC) and thermo-gravimetric analysis (TGA), respectively. Only the non-sulfonated PTFQ polymer showed  $T_g$  value at 176 °C in DSC.

The sulfonated PTFQSH-XX copolymers exhibit no glass transition temperature up to 350 °C. This may be due to the locking of segmental motion caused by inter-ionic interactions of sulfonic acid groups.

Thermal stabilities of the homopolymer and copolymers were examined in synthetic air at a heating rate of 10 K min<sup>-1</sup>. Fig. 3 shows the TGA plots of the polytriazoles (sulfonated and non-sulfonated) with different degree of sulfonation and the 10% weight loss temperatures are given in Table 2. The non-sulfonated polymer PTFQ showed single step degradation, on the other hand sulfonated copolymers exhibited three step degradation. The first step around 100 °C was due to the loss of the moisture absorbed by the membranes. The second weight loss around 195–235 °C was due the loss of the sulfonated groups, while the third weight loss around 253–328 °C was due to the degradation of the main chain backbone (triazole backbone). The main chain degradation temperatures of the PTFQSH-XX copolymers were higher than PTFQ homopolymer. This was attributed to the acid–base interactions of sulfonic acid group and the triazole ring in the PTFQSH-XX copolymers.

The polytriazole copolymers films showed very good mechanical properties in their acid and salt forms. The stress–strain plots of the salt form and acid form of dry sulfonated polytriazole copolymer membranes are shown in Fig. 4, and the mechanical properties are summarized in Table 2. The acidified polytriazole copolymer membranes showed higher tensile strength (42–60 MPa) and Young's modulus (1.64–2.01 GPa) in comparison to Nafion® 117 (tensile strength 22 MPa, Young's modulus 0.16 GPa) and previously reported analogous PTAQSH-XX series copolymers (tensile strength 8–53 MPa, Young's modulus 1.26–1.86 GPa) prepared from the non-fluorinated dialkyne monomer BPEBPA.<sup>21</sup>

However, these polymer membranes showed lower elongations at break (16–53%) compared to Nafion 117 (288%) due to the presence of rigid quadribiphenyl and hexa-fluoroisopropylidene moiety in the PTFQSH-XX.<sup>35</sup>

Durability of proton exchange membranes can be determined in terms of oxidative stability. The oxidative stability of the PTFQSH-XX membranes were studied as per reported protocol.<sup>30,34</sup> The polymer films (5 mm × 5 mm) were immersed into Fenton's reagent (2 ppm FeSO<sub>4</sub> in 3% H<sub>2</sub>O<sub>2</sub>) at 80 °C. The oxidative stability of the polymer membranes was determined

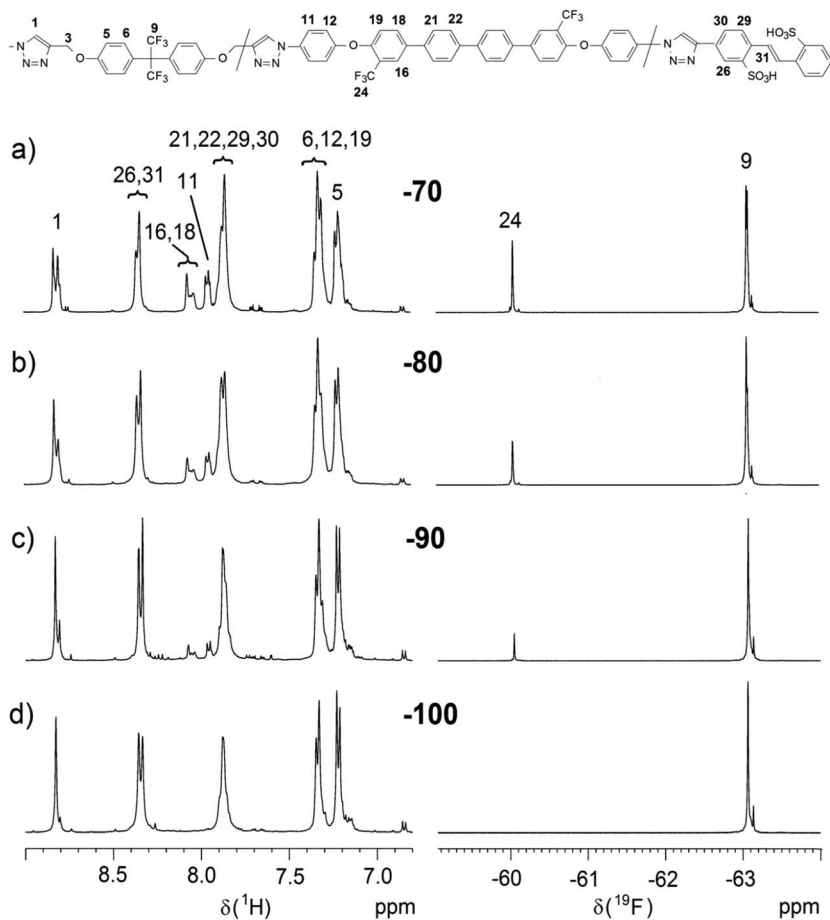


Fig. 2  $^1\text{H}$  NMR spectra (left, aromatic protons' region) and  $^{19}\text{F}$  NMR spectra (right) of PTFQSH-XX (XX = 70 (a), 80 (b), 90 (c); and PTFSH-100 (d)). Solvent:  $\text{DMSO-d}_6$  at  $60^\circ\text{C}$ . The structural fragment (top) specifies the atom numbering.

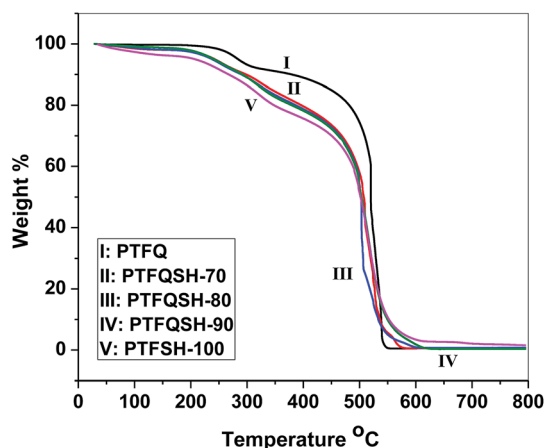


Fig. 3 TGA curves of the non-sulfonated and sulfonated polytriazoles.

by the time ( $\tau$ ) when the sample dissolved completely. Similar to the earlier report, the oxidative stability of PTFQSH-XX membranes decreases with increasing degree of sulfonation (Table 3). It is well known that the presence of  $>\text{C}(\text{CF}_3)_2$  groups in polymers improves many properties *e.g.* reduces water uptake and swelling ratio of the polymers and enhances the oxidative

stability.<sup>35</sup> Very strong electron withdrawing nature of  $>\text{C}(\text{CF}_3)_2$  groups that arises from the highest electron negativity of fluorine makes these polymers less susceptible to attack by the hydroxy and hydroperoxy radicals compared to the former reported polymers.<sup>21,35</sup> This was also attributed due to the formation less hydrated structures (low  $\text{IEC}_w$  value) of these polymers.<sup>31</sup> Thus, this series of copolymers showed improved oxidative stability in comparison to earlier reported BPEBPA based PTAQSH-XX copolymers with the same degree of sulfonation.<sup>21</sup> The PTFQSH-70 copolymer showed highest oxidative stability ( $\tau = >24$  h) whereas the copolymer PTFSH-100 showed lowest oxidative stability ( $\tau = 5$  h).

### 3.6. IEC (wet and volume based), water uptake, and swelling ratio

Ion exchange capacity plays a major role in PEMs, and it influences the water uptake and proton conductivity. The amount of the exchangeable protons in the dry ionic polymer is known as ion exchange capacity ( $\text{IEC}_w$ ), and it is directly proportional to the degree of sulfonation and inversely proportion to the molecular mass of the repeat unit of the polymer.

Table 2 Thermal and mechanical properties of PTFQS-XX polymers

Polymer	$T_g^a$ (°C)	10% wt loss temp. (°C)	Tensile strength (MPa)		Young modulus (GPa)		Elongation at break (%)	
	Acid form	Acid form	Salt form	Acid form	Salt form	Acid form	Salt form	Acid form
PTFQ	176	380	94.5 ± 1.9		2.38 ± 0.06		9.3 ± 1.1	
PTFQSH-70	n.d.	298	69.4 ± 1.6	58.2 ± 1.5	1.93 ± 0.03	2.01 ± 0.02	44.4 ± 2.2	34.4 ± 1.1
PTFQSH-80	n.d.	290	66.1 ± 1.2	60.3 ± 1.2	2.06 ± 0.06	1.95 ± 0.01	34.2 ± 0.8	53.2 ± 2.5
PTFQSH-90	n.d.	280	55.3 ± 1.6	49.2 ± 1.1	1.95 ± 0.02	1.93 ± 0.01	31.6 ± 0.3	20.2 ± 0.8
PTFSH-100	n.d.	267	50.4 ± 1.2	42.7 ± 1.5	1.81 ± 0.01	1.64 ± 0.02	17.8 ± 1.4	16.7 ± 1.5

<sup>a</sup> Glass transition temperature determined by DSC, n.d. – not detected.

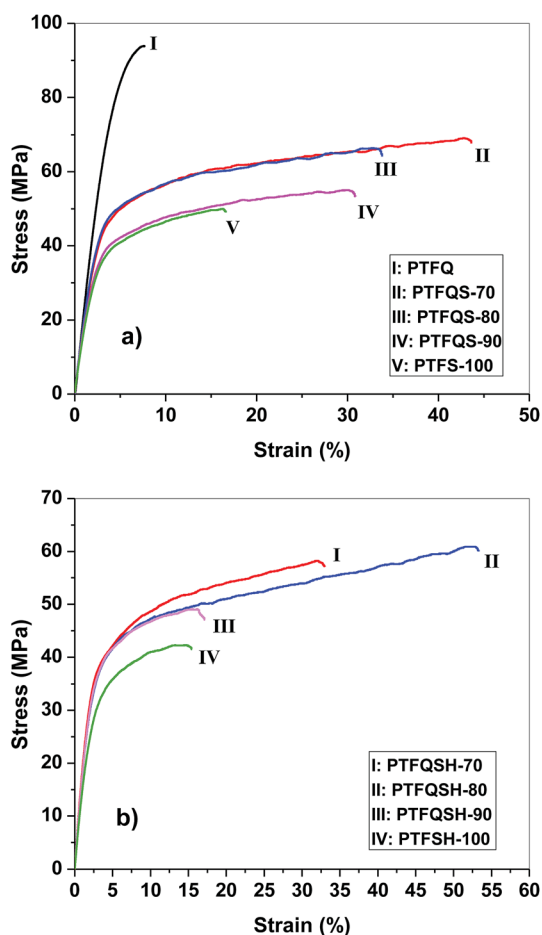


Fig. 4 Stress–strain plots for dry the polymeric membranes in (a) salt form and (b) acid form.

The main objective of this work was to study the effect of increasing fluorine content on the PEMs' properties. Accordingly, the PTFQSH-XX copolymers were prepared by replacing the non-fluorinated dialkyne monomer (BPEBPA) by the fluorinated dialkyne monomer (TF).<sup>21</sup> This resulted in the increase in percentage of fluorine from 0–5.61% to 13.66–16.10%, and consequent decrease in  $IEC_w$  from 1.72–2.75 to 1.52–2.40 meq  $g^{-1}$  (Tables 3 and 4) and that consequently affected many of the properties. The experimental  $IEC_w$  values of the membranes

were determined by titrimetry and calculated from the  $^1H$  NMR signal intensity. It can be found from Table 3, that these values harmonized with the theoretical values calculated from the molecular weight of the repeat unit of the copolymers. This indicates that the sulfonated monomer ("S") was successfully incorporated in the polymer *via* click polymerization. In PEMs weight-based ion exchange capacity ( $IEC_w$ , meq  $g^{-1}$ ) values are most frequently reported, though the volume based ion exchange capacity ( $IEC_v$ , meq  $g^{-1}$ ) values are more important (Table 3) to get a more accurate comparison of water uptake among different membranes. It is defined as the molar concentration of sulfonic acid groups per unit volume containing absorbed water.

The water uptake and the swelling ratio of the PEMs play a significant role on proton conductivity and mechanical properties. In sulfonated polymers hydrophilic sulfonic acid clusters are distributed in continuous hydrophobic domains and these hydrophilic regions are mainly responsible for water uptake. These hydrophilic regions absorb water and increase the cluster size into interconnecting channels for transport of protons, which in turn affects the proton conductivity and mechanical properties of PEMs. The weight based water uptake ( $WU_w$ ) and swelling ratio of the PTFQSH-XX membranes were determined from the changes in weight and length of the membranes at the required temperature and the values are shown in Tables 3 and 4. Similar to the previous study with PTAQSH-XX copolymers, it was observed that the water uptake ( $WU_w\%$ ) of PTFQSH-XX membranes increases continuously with increasing the  $IEC_w$  at a particular temperature (Fig. 5a and b).<sup>21</sup> The water uptake of PTFQSH-XX membranes were quite lower in comparison to the PTAQSH-XX membranes at all temperatures (Table 3) due to the higher fluorine content.<sup>21</sup>

The volume based water uptake ( $WU_v$ ) was evaluated by multiplying the density by wet based water uptake of the copolymer membranes. Similar to our previous study (PTAQSH-XX) the density of the PTFQSH-XX membranes decrease as fluorine percentage decreases and the degree of sulfonation increases. Also the densities of the PTFQSH-XX membranes are relatively higher in comparison to the corresponding PTAQSH-XX copolymers, which is also due to the higher fluorine content in the PTFQSH-XX polymers.<sup>21</sup>

Fig. 6a and b display the effect of  $IEC_v$ (dry) and  $IEC_v$ (wet) on the  $WU$  (vol%) of the PTFQSH-XX membranes. From the figures

Table 3 Density, IEC, water uptake and hydration number of PTFQSH-XX membranes

Polymer	$d_M^a$ (g cm <sup>-3</sup> )	IEC <sub>w</sub> (meq g <sup>-1</sup> )			IEC <sub>v</sub> <sup>d</sup> (meq g <sup>-1</sup> )			Water uptake <sup>e</sup> (wt%)		Water uptake <sup>f</sup> (vol%)		$\lambda^g$ [H <sub>2</sub> O/SO <sub>3</sub> ]	
		Theo. <sup>b</sup>	Titr.	NMR <sup>c</sup>	Wet			30 °C	80 °C	30 °C	80 °C	30 °C	80 °C
					Dry	30 °C	80 °C						
PTFQSH-70	1.46	1.52	1.50	1.52	2.22	1.98	1.90	8	12	12	17	3.06	4.26
PTFQSH-80	1.38	1.79	1.76	1.79	2.48	2.13	2.04	12	16	16	21	3.59	4.79
PTFQSH-90	1.34	2.09	2.04	2.00	2.77	2.31	2.08	15	30	21	39	4.06	7.92
PTFSH-100	1.30	2.40	2.36	2.40	3.12	2.34	2.13	26	42	33	54	5.95	9.67

<sup>a</sup> Density of membrane calculated from the weight and dimension of dry sample. <sup>b</sup> IEC<sub>w, Theo.</sub> = (1000/ $M_w$  repeat unit) × DS<sub>Theo.</sub> × 2, where DS<sub>Theo.</sub> is calculated theoretically from monomer feed ratio. <sup>c</sup> IEC<sub>w, NMR</sub> = (1000/ $M_w$  repeat unit) × DS<sub>NMR</sub> × 2, where DS<sub>NMR</sub> is calculated from NMR peak ratio. <sup>d</sup> IEC<sub>v</sub>(dry) = (IEC<sub>w, Theo.</sub>) ×  $d_M$  and IEC<sub>v</sub>(wet) = IEC<sub>v</sub>(dry)/(1 + 0.01WU). <sup>e</sup> WU(wt%) = [( $W_{wet} - W_{dry}$ )/ $W_{dry}$ ] × 100. <sup>f</sup> WU(vol%) = [( $W_{wet} - W_{dry}$ )/ $d_w$ ]/( $W_{dry}/d_M$ ) × 100. <sup>g</sup>  $\lambda$  = WU<sub>w</sub> (%) / (100 × IEC<sub>w, Theo.</sub> ×  $M_w$ , H<sub>2</sub>O), where  $M_w$ , H<sub>2</sub>O = 18 g mol<sup>-1</sup>.

it is evident that the volume based IECs [IEC<sub>v</sub>(dry) and IEC<sub>v</sub>(wet)] showed a similar trend at 30 °C when both of them were plotted against WU (vol%). However, IEC<sub>v</sub>(wet) displays broad deviation in comparison to the IEC<sub>v</sub>(dry) at 80 °C, that was due to the percolation effect. That effect was significant for these copolymers after reaching a certain IEC<sub>v</sub>(wet) value.

The in-plane ratio and through-plane swelling ratio of the PTFQSH-XX membranes were determined by the changes in length and thickness at the experimental temperature and the results are shown in Table 4. The in-plane swelling ratio of the PTFQSH-XX membranes were found to be lower in comparison to the PTAQSH-XX polymers and Nafion®117.<sup>21</sup> This was due to the presence of the hydrophobic rigid quadribiphenyl and aromatic triazole moieties in the PTFQSH-XX membranes along with high fluorine content. Fig. 7 displays through plane swelling ratio with a degree of sulfonation at temperatures of investigation.

### 3.7. Wide angle X-ray diffraction analysis

The wide angle X-ray diffraction (WAXD) patterns of the poly-triazole films was recorded at room temperature and are shown in Fig. 8. The PTFQ, PTFQSH-80, and PTFQSH-90 (in dry state), and PTFQSH-90 (in wet state) polytriazoles display several amorphous halos (21.34° for PTFQ<sub>dry</sub>, 23.35° for PTFQSH-80<sub>dry</sub>, 24.87° for PTFQSH-90<sub>dry</sub> and 24.08° for PTFQSH-90<sub>wet</sub>). From the diffractogram of the polymers, it is apparent that all the polymers are amorphous in nature. This is due to the presence

of flexible ether linkage and hexafluoroisopropylidene moiety in the polymer backbone that hindered the ordered arrangement of the polymer packing.<sup>35,36</sup> When sulfonic acid and triazole interactions were present in the polymers, the characteristic amorphous peak (PTFQ = 21.34°) was shifted to higher values (PTFQSH-80<sub>dry</sub> = 23.35° and PTFQSH-90<sub>dry</sub> = 24.87°). Also the characteristic amorphous halo of PTFQSH-90<sub>dry</sub> was shifted to a lower value (PTFQSH-90<sub>wet</sub> = 24.08°). This is due to the formation of the larger ionic clusters in the dry membrane after the water absorption.

### 3.8. Microstructural analysis

The microstructure of the membranes plays an important role in the proton conduction and mechanical stability. The microstructure of the PTFQSH-XX membranes were studied by transmission electron microscope, and TEM micrographs are shown in the Fig. 9. In order to understand the phase separation and ionic aggregation of the membranes, the polytriazole membranes were stained by lead acetate. The black spherical regions in the micrographs are due to the association of lead ions exchanged with the sulfonic acid groups, which represent the hydrophilic domains. The brighter regions in the micrographs correspond to the hydrophobic domains in the membranes. The TEM image of PTFQSH-70 membrane showed small size ionic domains (3–10 nm) dispersed throughout the hydrophobic region. PTFQSH-80 forms a microphase separated structure with a large number of medium size ionic domains

Table 4 Dimensional swelling, oxidative stability and proton conductivity of PTAQSH-XX copolymers

Polymer	Elemental F (%)	Swelling ratio (%)				Oxidative stability <sup>a</sup> (h)	$\sigma$ (mS cm <sup>-1</sup> )		$E_a^b$ (kJ mol <sup>-1</sup> )
		In plane		Through plane			30 °C	80 °C	
		30 °C	80 °C	30 °C	80 °C				
PTFQSH-70	16.10	n.d.	n.d.	4	9	>24	9	27	20.90
PTFQSH-80	15.34	n.d.	n.d.	9	15	>24	13	46	22.83
PTFQSH-90	14.52	n.d.	n.d.	16	23	18	30	86	19.53
PTFSH-100	13.66	4.76	9.09	23	35	5	54	136	16.23
Nafion® 117	n.d.	11	n.d.	19	n.d.	n.d.	60	135	13.65

<sup>a</sup> The complete dissolution time in Fenton's reagent (2 ppm FeSO<sub>4</sub> in 3% H<sub>2</sub>O<sub>2</sub>) at 80 °C. <sup>b</sup> Activation energy determined in the temperature range 30–80 °C and heating rate 1–2 K min<sup>-1</sup>.

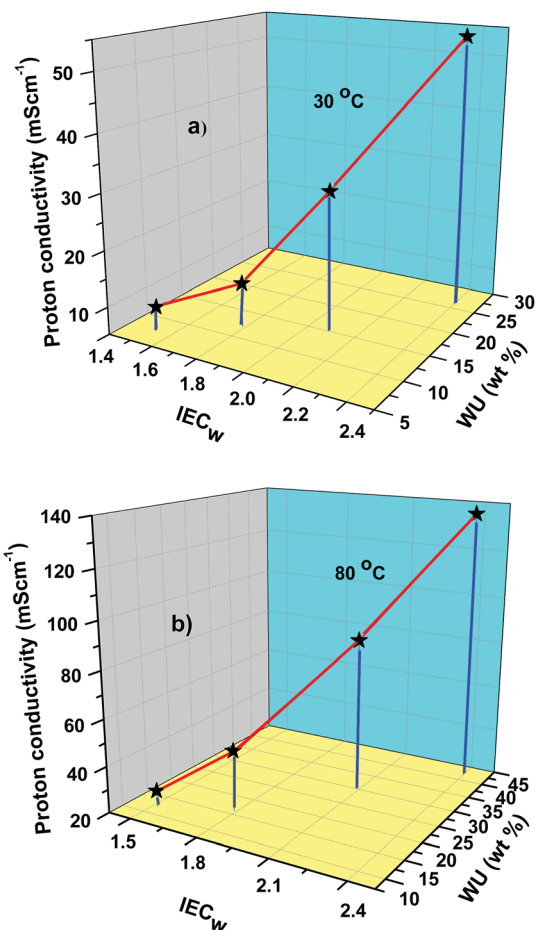


Fig. 5 Correlation plot of IEC<sub>w</sub>, WU (wt%) and proton conductivity of PTFQSH-XX membranes (a) at 30 °C and (b) at 80 °C.

(25–35 nm). However, larger ionic domains (40–75 nm) were observed in the case of PTFQSH-90 and PTFQSH-100 membranes.

It is obvious from the TEM micrographs of PTFQSH-XX membranes that the size of the ionic domains regularly increases with increasing the degree of sulfonation. The highly hydrophobic character of hexafluoroisopropylidene and quadribiphenyl moieties in the PTFQSH-XX membranes facilitates to form ionic clusters of microphase separated morphology.

### 3.9. Proton conductivity

Proton conductivity is the most important property of the proton exchange membranes used in fuel cells. Before doing the experiment, the acidified membranes were kept in deionized water for 72 h at room temperature to achieve full hydration. In-plane proton conductivity of the PTFQSH-XX membranes were measured in deionized water by using electrochemical impedance spectroscopy. The membrane resistance was obtained from Nyquist diagram from the high-frequency intercept of the characteristic semicircle in the real axis. The Nyquist diagrams of PTFQSH-XX membranes are shown in Fig. 10a and b. The resistance values of the polytriazole membranes decrease with increasing temperature. Fig. 10a shows a representative Nyquist diagram for PTFQSH-70 copolymer at temperatures from 30–90 °C.

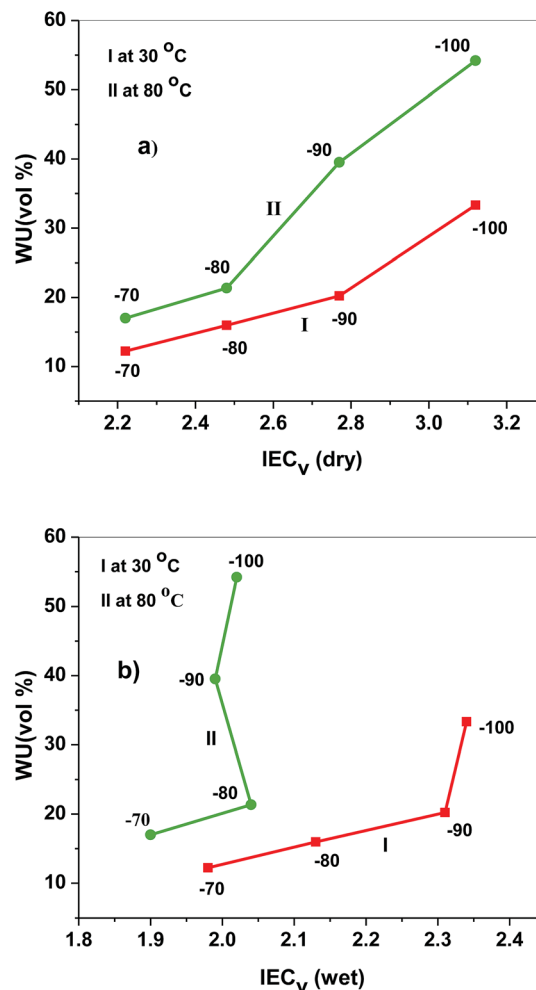


Fig. 6 Water uptake (vol%) dependence of IEC<sub>v</sub>(dry), and IEC<sub>v</sub>(wet) values of PTFQSH-XX membranes.

In fixed temperature, the resistance values of the polytriazole membranes also decrease with increasing DS values (Fig. 10b). The proton conductivities of the PTFQSH-XX membranes were

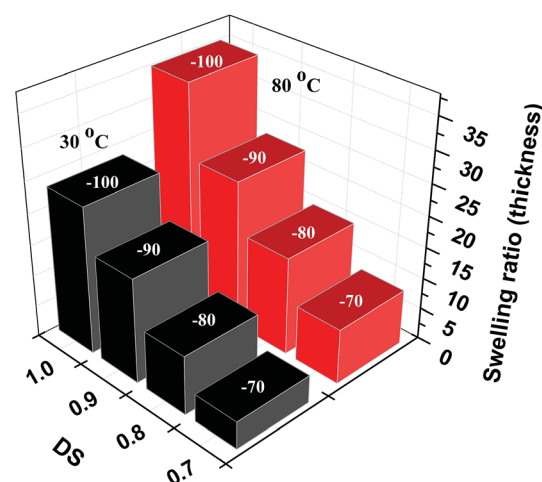


Fig. 7 Through-plane swelling ratio (thickness) of PTFQSH-XX membranes of different degrees of sulfonation (DS) at 30 °C and 80 °C.

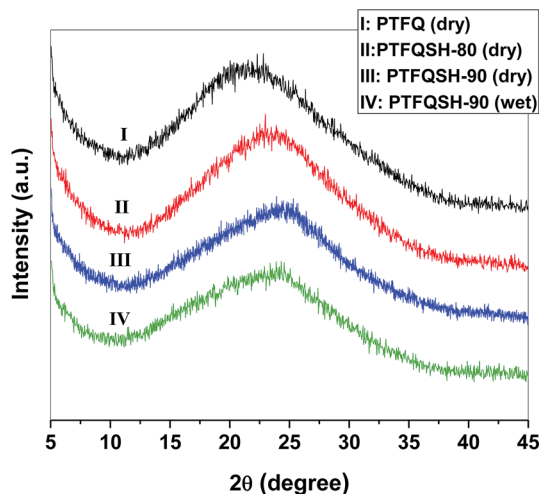


Fig. 8 XRD diffractogram of dry PTFQ, PTFQSH-80 and PTFQSH-90, and wet state PTAQSH-90 membranes.

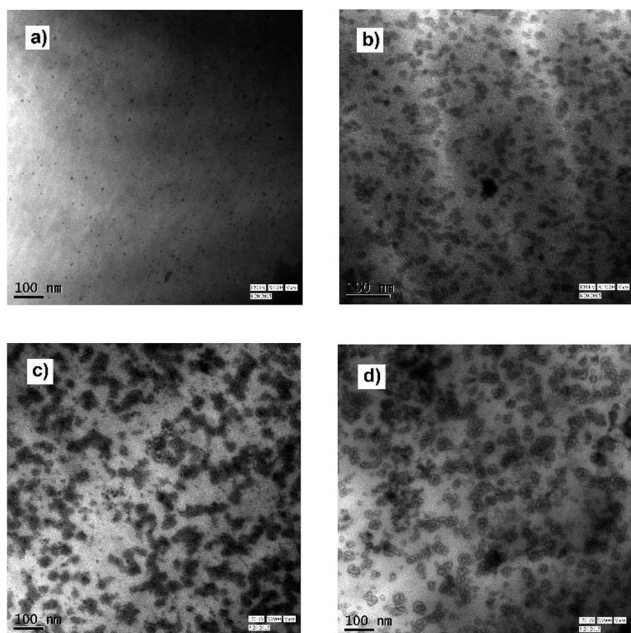


Fig. 9 TEM micrographs of lead ( $\text{Pb}^{2+}$ ) stained PTFQSH-XX (XX = 70 (a), 80 (b), 90 (c); and PTFSH-100 (d)) copolymers.

found to be in the range of  $9\text{--}54\text{ mS cm}^{-1}$  at  $30\text{ }^\circ\text{C}$ , and  $27\text{--}136\text{ mS cm}^{-1}$  at  $80\text{ }^\circ\text{C}$  (Table 4). The proton conductivity of PTFQSH-70 membrane was lower in comparison to the PTAQSH-70 membrane.<sup>21</sup> This may be due the lower water uptake and lower  $\text{IEC}_w$  value of PTFQSH-70 membrane. However, the proton conductivities of PTFQSH-80, PTFQSH-90 and PTFSH-100 membranes were higher in comparison to the analogues PTAQSH-XX membranes with same DS values. The proton conductivity of PTFQSH-90 membrane ( $86\text{ mS cm}^{-1}$  at  $80\text{ }^\circ\text{C}$ ) was higher in comparison to the similar  $\text{IEC}_w$  containing PTAQSH-80 copolymer ( $47\text{ mS cm}^{-1}$  at  $80\text{ }^\circ\text{C}$ ), also the PTFSH-100 membrane ( $136\text{ mS cm}^{-1}$  at  $80\text{ }^\circ\text{C}$ ) showed much higher

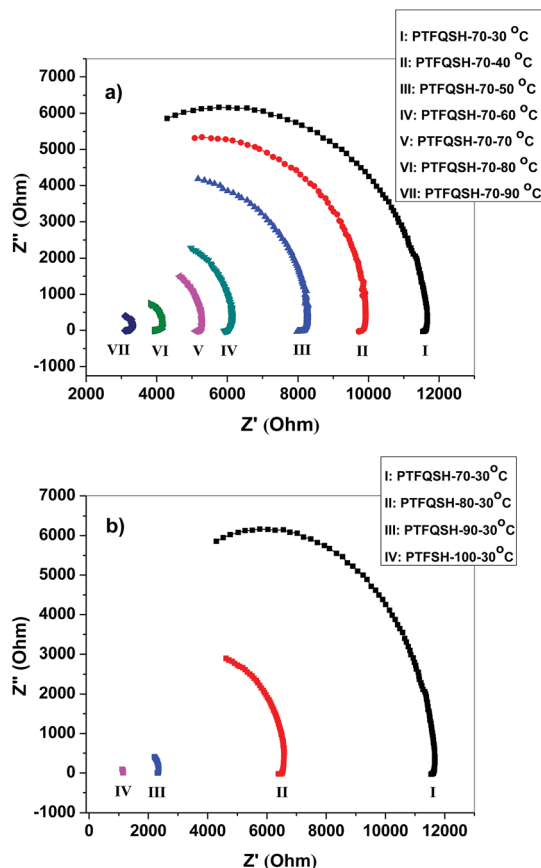


Fig. 10 Variation in the impedance behavior of the PTFQSH-XX membranes with (a) temperature at fixed composition and (b) composition at  $30\text{ }^\circ\text{C}$ ;  $Z'$ , the real part of impedance and  $Z''$ , the imaginary part of the impedance.

proton conductivity in comparison to the similar  $\text{IEC}_w$  containing sulfonated polytriazole copolymers PTAQSH-90 ( $76\text{ mS cm}^{-1}$  at  $80\text{ }^\circ\text{C}$ ) and PTA1 ( $72\text{ mS cm}^{-1}$  at  $80\text{ }^\circ\text{C}$ ).<sup>19,21</sup> This is attributed to the better phase separation and interconnected hydrophilic domains in the PTFQSH-XX membranes. When the

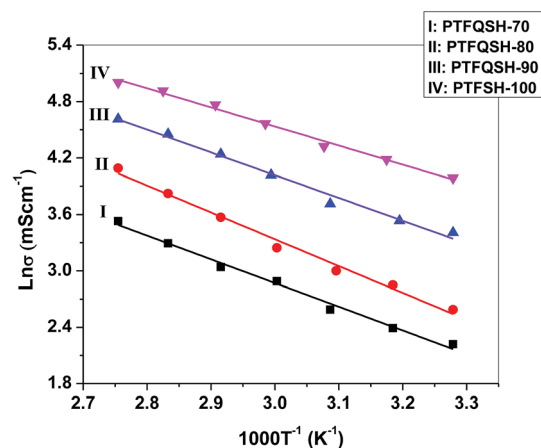


Fig. 11 Arrhenius type temperature dependent proton conductivity ( $\sigma$ ) behavior of PTFQSH-XX membranes.

ratios of proton conductivity per water uptake (vol%) values were considered, the PTFQSH-XX displays higher values in comparison to PTAQSH-XX membranes, which shows better management of water in the enhancement of the proton conductivity.

The Arrhenius plots of the PTFQSH-XX membranes were used to investigate the temperature dependence of the proton conductivity (Fig. 11), and the activation energy ( $E_a$ ) for the proton conductivity of the polytriazole membranes was calculated according to the procedure reported in literature.<sup>30</sup> The activation energies of the PTFQSH-XX membranes were found to be in the range of 22.83–16.23 kJ mol<sup>-1</sup>, which was close to the reported value of Nafion® 117 and other sulfonated polymers.<sup>21</sup>

## 4. Conclusion

A new series of highly fluorinated sulfonated polytriazoles (PTFQSH-XX) with a controlled degree of sulfonation were synthesized by azide-alkyne click polymerization. The PTFQSH-XX copolymers were converted into flexible membranes by using solution casting method. The structures of the polytriazole copolymers were confirmed by FTIR and <sup>1</sup>H, <sup>13</sup>C, and <sup>19</sup>F NMR spectroscopic studies. The ion exchange capacities of the copolymers were determined from titrimetry and <sup>1</sup>H NMR analysis and matched nicely with the monomer feed ratio. The use of rigid hexafluoroisopropylidene and quadribiphenyl moieties in the main chain played major role in realizing good thermal stability and high mechanical strength. The copolymers showed 10% decomposition temperature in the range of 267–380 °C. The tensile strength of the PTFQSH-XX membranes were found to be in the range of 42–60 MPa, which was much higher than that of Nafion®117 (22 MPa) and many other sulfonated copolymers. The membranes from PTFQSH-XX copolymers showed lower water uptake, lower swelling and relatively higher oxidative stability in comparison to the analogous PTAQSH-XX based membranes, which is due to the higher fluorine content in the PTFQSH-XX based copolymers. The presence of highly hydrophobic -CF<sub>3</sub> and >C(CF<sub>3</sub>)<sub>2</sub> moieties in the high DS polymers creates a polarity difference in hydrophilic and hydrophobic segments in the polymer due to which PTFQSH-XX copolymers showed better phase separated morphology and high proton conductivity (27–136 mS cm<sup>-1</sup> at 80 °C). The PTFQSH-90 is the best in the series considering its overall membrane properties like, oxidative stability (18 h), thermal (10% weight degradation temperature = 280 °C) and mechanical stability (tensile strength = 49 MPa and young modulus = 1.93 GPa), proton conductivity (86 mS cm<sup>-1</sup> at 80 °C) and dimensional stability.

## Acknowledgements

A. Singh thank to the Council of Scientific and Industrial Research, New Delhi, India for providing the fellowship to carry out this work. The authors thank Ms Ch. Harnisch and Dr A. Lederer (IPF Dresden) for GPC analysis of the polymers.

## References

- 1 M. A. Hickner, H. Ghassemi, Y. S. Kim, B. R. Einsla and J. E. McGrath, *Chem. Rev.*, 2004, **104**, 4587.
- 2 H. Zhang and P. K. Shen, *Chem. Soc. Rev.*, 2012, **41**, 2382.
- 3 Y. Chikashige, Y. Chikyu, K. Miyatake and M. Watanabe, *Macromolecules*, 2005, **38**, 7121.
- 4 J. K. Lee, W. Li and A. Manthiram, *J. Membr. Sci.*, 2009, **330**, 73.
- 5 C. Wang, N. Li, D. W. Shin, S. Y. Lee, N. R. Kang, Y. M. Lee and M. D. Guiver, *Macromolecules*, 2011, **44**, 7296.
- 6 G. Li, C. Zhao, X. Li, D. Qi, C. Liu, F. Bu and H. Na, *Polym. Chem.*, 2015, **6**, 5911.
- 7 P. Xing, G. P. Robertson, M. D. Guiver, S. D. Mikhailenko and S. Kaliaguine, *Macromolecules*, 2004, **37**, 7960.
- 8 P. Xing, G. P. Robertson, M. D. Guiver, S. D. Mikhailenko and S. Kaliaguine, *Polymer*, 2005, **46**, 3257.
- 9 K. Shao, J. Zhu, C. Zhao, X. Li, Z. Cui, Y. Zhang and W. Xing, *J. Polym. Sci., Part A: Polym. Chem.*, 2009, **47**, 5772.
- 10 M. D. T. Nguyen, H. S. Dang and D. Kim, *J. Membr. Sci.*, 2015, **496**, 13.
- 11 K. Miyatake, H. Zhou, T. Matsuo, H. Uchida and M. Watanabe, *Macromolecules*, 2004, **37**, 4961.
- 12 K. Yamazaki and H. Kawakami, *Macromolecules*, 2010, **43**, 7185.
- 13 Z. Zhang and T. Xu, *J. Mater. Chem. A*, 2014, **2**, 11583.
- 14 H. Yao, P. Feng, P. Liu, B. Liu, Y. Zhang, S. Guan and Z. Jiang, *Polym. Chem.*, 2015, **6**, 2626.
- 15 S. Kang, C. Zhang, G. Xiao, D. Yan and G. Sun, *J. Membr. Sci.*, 2009, **334**, 91.
- 16 J. A. Mader and B. C. Benicewicz, *Macromolecules*, 2010, **43**, 6706.
- 17 L. Sheng, H. Xu, X. Guo, J. Fang, L. Fang and J. Yin, *J. Power Sources*, 2011, **196**, 3039.
- 18 I. I. Ponomarev, M. Y. Zharinova, P. V. Petrovskii and Z. S. Klemenkova, *Dokl. Chem.*, 2009, **429**, 305.
- 19 Y. J. Huang, Y. S. Ye, Y. C. Yen, L. D. Tsai, B. J. Hwang and F. C. Chang, *Int. J. Hydrogen Energy*, 2011, **36**, 15333.
- 20 Y. J. Huang, Y. S. Ye, Y. J. Syu, B. J. Hwang and F. C. Chang, *J. Power Sources*, 2012, **208**, 144.
- 21 A. Singh, R. Mukherjee, S. Banerjee, H. Komber and B. Voit, *J. Membr. Sci.*, 2014, **469**, 225.
- 22 H. C. Kolb, M. G. Finn and K. B. Sharpless, *Angew. Chem.*, 2001, **40**, 2004.
- 23 J. E. Moses and A. D. Moorhouse, *Chem. Soc. Rev.*, 2007, **36**, 1249.
- 24 V. V. Rostovtsev, L. G. Green, V. V. Fokin and K. B. Sharpless, *Angew. Chem.*, 2002, **114**, 2708.
- 25 R. X. Yao, L. Kong, Z. S. Yin and F. L. Qing, *J. Fluorine Chem.*, 2008, **129**, 1003.
- 26 K. A. Smith, Y. H. Lin, D. B. Dement, J. Strzalka, S. B. Darling, D. L. Pickel and R. Verduzco, *Macromolecules*, 2013, **46**, 2636.
- 27 I. Dimitrov, S. Takamuku, K. Jankova, P. Jannasch and S. Hvilsted, *J. Membr. Sci.*, 2014, **450**, 362.
- 28 W. Wu, Z. Wang, R. Xiao, Z. Xu and Z. Li, *Polym. Chem.*, 2015, **6**, 4396.

- 29 T. Ko, K. Kim, B. K. Jung, S. H. Cha, S. K. Kim and J. C. Lee, *Macromolecules*, 2015, **48**, 1104.
- 30 A. K. Mohanty, E. A. Mistri, A. Ghosh and S. Banerjee, *J. Membr. Sci.*, 2012, **409**, 145.
- 31 A. K. Mohanty, E. A. Mistri, S. Banerjee, H. Komber and B. Voit, *Ind. Eng. Chem. Res.*, 2013, **52**, 2772.
- 32 J. Pang, X. Jin, Y. Wang, S. Feng, K. Shen and G. Wang, *J. Membr. Sci.*, 2015, **492**, 67.
- 33 K. S. Kumar, B. Sreelakshmi and C. R. Nair, *Mater. Lett.*, 2014, **137**, 315.
- 34 S. Zhong, X. Cui, H. Cai, T. Fu, C. Zhao and H. Na, *J. Power Sources*, 2007, **164**, 65.
- 35 S. Banerjee, *Handbook of Specialty Fluorinated Polymers*, Elsevier, 1<sup>st</sup> edn, 2015, ch. 1–6, pp. 1–329, ISBN: 9780323357920.
- 36 P. Bandyopadhyay, D. Bera and S. Banerjee, *J. Membr. Sci.*, 2011, **382**, 20.